Metal–organic polyhedron from a flexible tetrakis(thiobenzyl-carboxylate)-tetrathiafulvalene

Yohan Cheret, Narcis Avarvari, Nicolas Zigon

Metal-organic polyhedron from a flexible tetrakis(thiobenzyl-carboxylate)-Tetrathiafulvalene

Yohan Cheret,[1] Narcis Avarvari,*[,1] Nicolas Zigon*[,1]

[1] Univ Angers, CNRS, MOLTECH-ANJOU, SFR MATRIX, F-49000 Angers, France. E-mail: narcis.avarvari@univ-angers.fr; nicolas.zigon@univ-angers.fr

Table of content

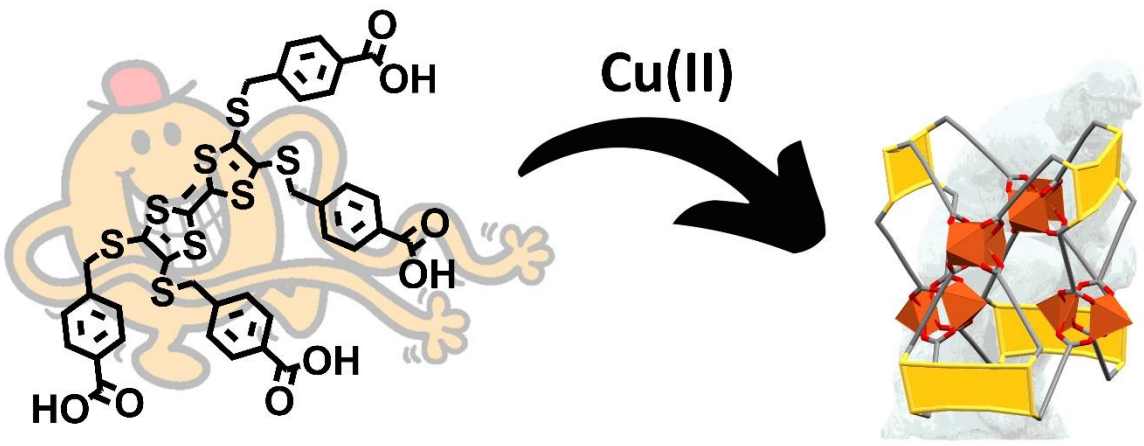

Wiggle, wiggle… Stay! A redox-active tetrakis(thiobenzyl-carboxylate)-TTF with a high degree of flexibility stands still in a self-assembled cage upon complexation with Cu(II).

Keywords

Metal-Organic Polyhedra

Crystal engineering

Tetrathiafulvalene

Cyclic voltammetry

X-ray diffraction

ABSTRACT

The synthesis of crystalline self-assembled materials starting from building blocks with a large degree of freedom is challenging. Furthermore, incorporating redox-active moieties in self-assembled metal-organic polyhedra is of the outmost interest to modulate the properties of the cavity through redox stimuli. Herein is presented the synthesis of a novel electroactive ligand bearing four coordinating moieties around an S-alkylated tetrathiafulvalene (TTF) scaffold. The redox behavior of the ligand is similar to a tetra-S-alkylated TTF. In the solid state, it presents a densely packed H-bonded 1D polymeric structure. Upon reaction with $Cu(OAc)_2$ in the presence of dimethylformamide or dimethylacetamide, two novel M_4L_4-type metal-organic polyhedra (MOPs) bearing paddlewheel metal clusters as connecting nodes are obtained. The structural features and electrochemical properties of the ligand and the MOPs are devised. Both MOPs adopt the same structure characterized by a tetrahedral arrangement of the four TTF moieties.

The concept of self-assembly arose with supramolecular chemistry in the 60s and the description of the recognition abilities of covalent macrocycles such as crown ethers or cryptands.[1–3] Various viruses or cargo proteins exhibit highly-ordered geometrical shapes.[4,5] The use of reversible interactions such as hydrogen bonds or van der Waals interactions to construct structures through the assembly of topologically well-defined building blocks is an efficient mean to access supramolecules with a higher complexity or novel physical properties.[6] Amongst these, the coordination cages – also known as metal-organic polyhedra (MOP) – are formed through the combination of a polytopic divergent coordination linker and a metal or metal cluster.[7,8] One of the most frequently encountered secondary building unit are the metal paddlewheel clusters composed of anionic carboxylates and metals (commonly Cu(II),[9] Rh(II),[10] Cr(II)[11] or Mo(II)[12]). Their porosity, their stability in various media and their ease of functionalization on the organic moieties makes them excellent candidates for catalysis,[13,14] for ion transport,[15] drug-delivery,[16] or gas sorption.[10,17,18] Encompassing the cages with redox-active functionalities makes them stimuli responsive and could lead to a variation of their encapsulation abilities. In that regard, the use of electron-rich moieties such as tetrathiafulvalene (TTF) in combination with various coordinating units, has been thoroughly explored as well in self-assembled systems for guest encapsulation.[19–21] Macrocyclic fully organic species using S-alkylated TTF have been described,[22–24] but to the best of our knowledge not incorporated in metal-organic cages despite their easy synthetic availability.

Furthermore, the flexibility of the cage is a key factor for proper guest enclathration.[25,26] Most of the ligands used in metal-organic cages design have nevertheless highly restrained degrees of freedom.

In this communication is described the straightforward synthesis of a large and flexible TTF-tetrakis(thiobenzyl-carboxylic) acid. The redox properties of the S-alkyl TTF core are retained upon functionalization. The self-assembly of the tetracarboxylic acid with Cu(II) affords M_4L_4-type metal-organic cages that were structurally characterized by single crystal X-ray diffraction (SCXRD).

The starting material 3,3',3'',3'''-([2,2'-bi(1,3-dithiolylidene)]-4,4',5,5'-tetrayltetrakis(sulfanediyl))tetrapropanenitrile (**1**) was prepared using classical phosphite mediated coupling.[27] The synthesis was done in two steps to obtain the desired target ligand **L** (**Scheme 1**) further used to prepare the **TTF-CuMOP** described herein (*vide infra*). In a first step, the propionitrile protecting groups are removed in basic media to generate a tetrathiolate, followed by the addition of the methyl 4-(bromomethyl)benzoate, affording the intermediate **2** with an 83 % yield. This compound is then saponified in a basic aqueous media to yield after re-acidification the tetraacid **L** with 84 % yield. Noteworthy, a TTF-tetrakis(4-picolylthio) was reported for the construction of metallamacrocycles and 1-D coordination polymers.[28]

The flexibility is defined by Furukawa, Fujita *et coll.* as "*the number of rotatable bonds in the main scaffold*" for a given ligand,[8] and reaches 12 for **L** (3 rotatable bonds between the TTF core and each benzoic acid moiety). This makes **L** the most flexible carboxylate based ligand ever reported to form a cage to the best of our knowledge.

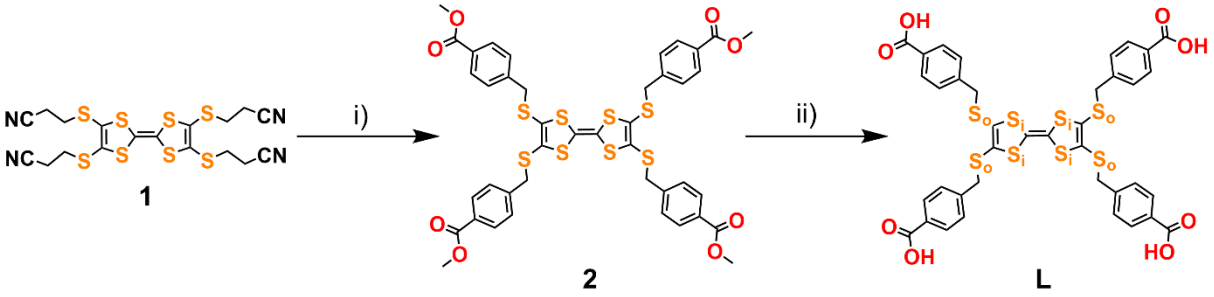

Scheme 1. Synthetic route to **L**. i) Na, EtOH, methyl 4-(bromomethyl)benzoate, RT, overnight (83%) ; ii) NaOH, THF/MeOH/H_2O, 80°C, overnight, then HCl 10%, RT (84%). S_i and S_o stand for inner and outer sulfur atoms, respectively, in **L**.

Electrochemical properties of **2** and **L** were investigated by cyclic voltammetry. In both cases two reversible oxidations waves are observed (**Figure 1**, **2** : $E_1^{1/2}$ = + 0.55 V, $E_2^{1/2}$= + 0.72 V and **L** : $E_1^{1/2}$ = + 0.55 V, $E_2^{1/2}$= + 0.72 V vs. SCE). The reference compound tetramethylthio-TTF (TMT-TTF) is described in the literature with values of : $E_1^{1/2}$ = + 0.51 V, $E_2^{1/2}$= + 0.78 V vs SCE.[29] Neither the presence of benzoic ester nor the acids have therefore a stringent impact on the redox activity of the ligand.

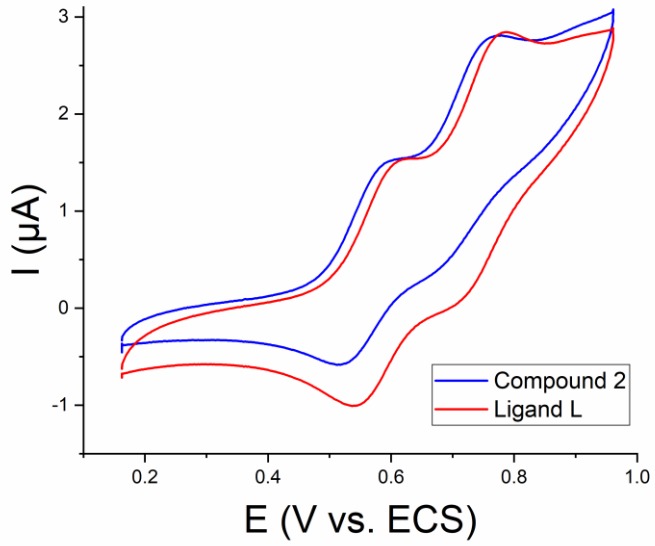

Figure 1. Cyclic voltammograms recorded between 0.1 and 1.0 V for a solution in 0.1 M $TBAPF_6$ in DMF. Scan rate: 100 $mV.s^{-1}$.

Suitable crystals of **L** for X-ray structural determination were obtained by slow evaporation of a DMSO solution (**Figure 2**). The ligand crystallizes as orange plates in the monoclinic space group $P2_1/c$. The asymmetric unit contains half of a neutral ligand molecule and one disordered DMSO molecule. The central C=C bond is 1.338(5) Å long, which is in accordance with a non-oxidized TTF.[30] Each DMSO molecule connects two carboxylic acids from two different molecules of **L** through H-bonding with 2.652(7) and 2.98(1) Å intermolecular O_L-O_{DMSO} distances. Two benzoic acids located on the same fulvalene moieties are associated through these DMSO mediated H-bonds to two benzoic acid moieties of an adjacent molecule of **L**. This creates an infinite one-dimensional H-bonded polymer (**Figure 2c**) where the TTF moieties are repeating every 22.701(5) Å. TTF-tetrabenzoic acid was already reported to yield hydrogen-bonded frameworks with conductivities in the 10^{-7}-10^{-6} S/cm range.[31,32] The 1-D strands are further interconnected through lateral S···H-C bonds. Noteworthy, two TTF moieties from two different strands lies in a shifted fashion. We define the inner and outer sulfur atoms as S_i and S_o, respectively (see **Scheme 1**). The S_i-S_i intermolecular bond distances are 4.231(2) and 4.292(1) Å while the S_o-S_i intermolecular bond distances are 4.196(1), 4.532(2), 4.548(1) and 4.851(2) Å long.

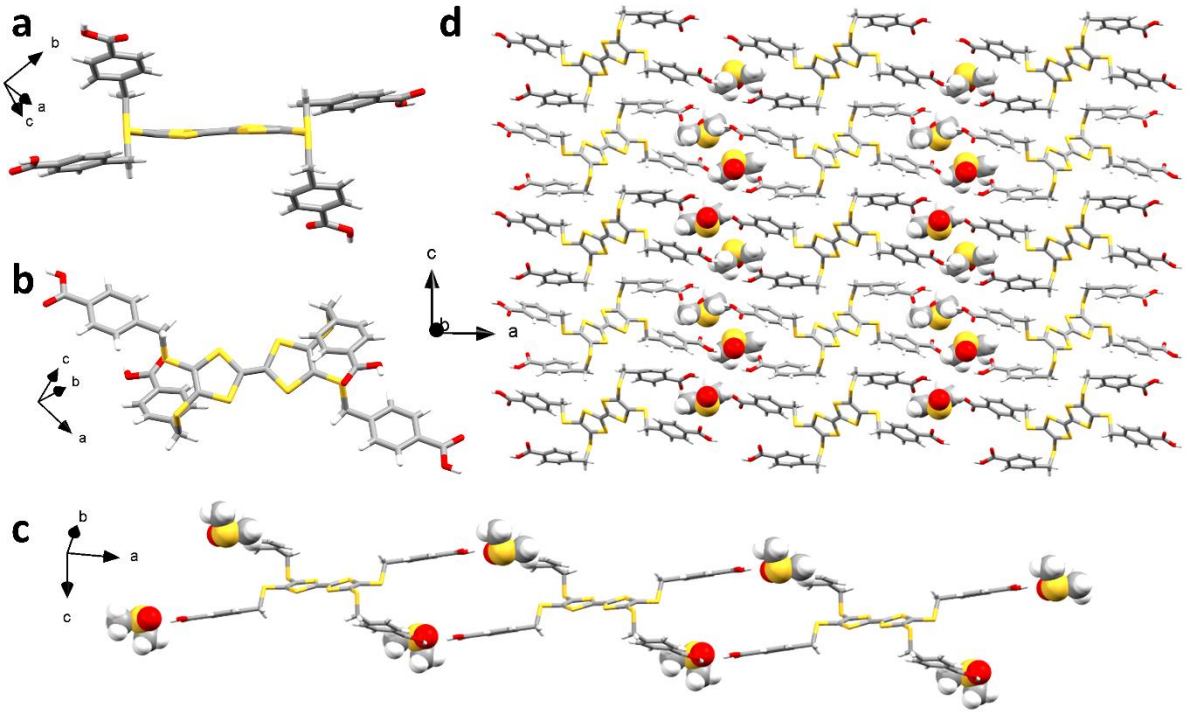

Figure 2. X-ray crystal structure of the compound **L**. a) Side and b) top views of the ligand **L**. c) View of the one-dimensional H-bonded polymer and d) view of the complete packing along the *b*-axis. DMSO solvent molecules are represented as space fillings, and disordered molecules were removed for the sake of clarity (Carbon: grey ; Oxygen : red ; Sulfur : yellow ; Hydrogen : white).

Suitable crystals for SCXRD for the self-assembled cages **Cu_8L_4-(DMAc)** and **Cu_8L_4-(DMF)** were obtained by using the solvothermal method in carefully layered solutions of the ligand and $Cu(OAc)_2$ in dimethylacetamide (DMAc) or dimethylformamide (DMF). **Cu_8L_4-(DMAc)** crystallized as green needles in the triclinic space group (*P*-1) with the complete formula **$Cu_8L_4(DMAc)_6(H_2O)_2 \cdot(DMAc)_{4.48}$**. The asymmetric unit displays one full cage with four TTF units connected by four Cu(II) paddle-wheel clusters (**Figure 3a**, TTF moieties in yellow ; metal paddlewheel in orange). The four apical positions pointing outside of the MOP are occupied by DMAc molecules. In the more sterically constrained inner apical positions, two sites are occupied by H_2O molecules, and the two others by DMAc molecules. No strong intra- or inter-ligand interactions were observed within the cage, and therefore the H-bonds formed by the inner apical H_2O and DMAc solvent molecules should have a templating role in the self-assembly of the structure. The central C=C bonds of the TTF moieties lies in the 1.26(2) – 1.34(2) Å range. Furthermore, no counter-ions were found in the structure, which hints at a neutral form of the TTF moiety.

In addition to the coordinated solvent molecules, five non-coordinated DMAc were found in the unit cell. Two DMAc involved in H-bonding with the inner apical H_2O molecules have refined occupancies of 100% and 63% (d_{O-O} in the 2.75-2.96 Å range) and are located inside of the cage. Five additional DMAc molecules lie outside of the MOP in the crystal structure, with refined occupancies of 100, 60, 50, 40 and 35%. They interact through H-bonding and van der Waals interactions with the cages. The aromatic moieties form V-shaped surfaces with angles of 82° and 90° (**Figure 3b and c**).

As can be seen in **Figure 3d**, the cages pack in a head-to-tail fashion. DMAc molecules located outside of the cavities are filling the void spaces between the V-shaped aromatic planes. Noteworthy, only one layer of **Cu_8L_4-(DMAc)** is represented on **Figure 3d**. Adjacent layers do not define 1D channels but enclose the spaces between the cages.

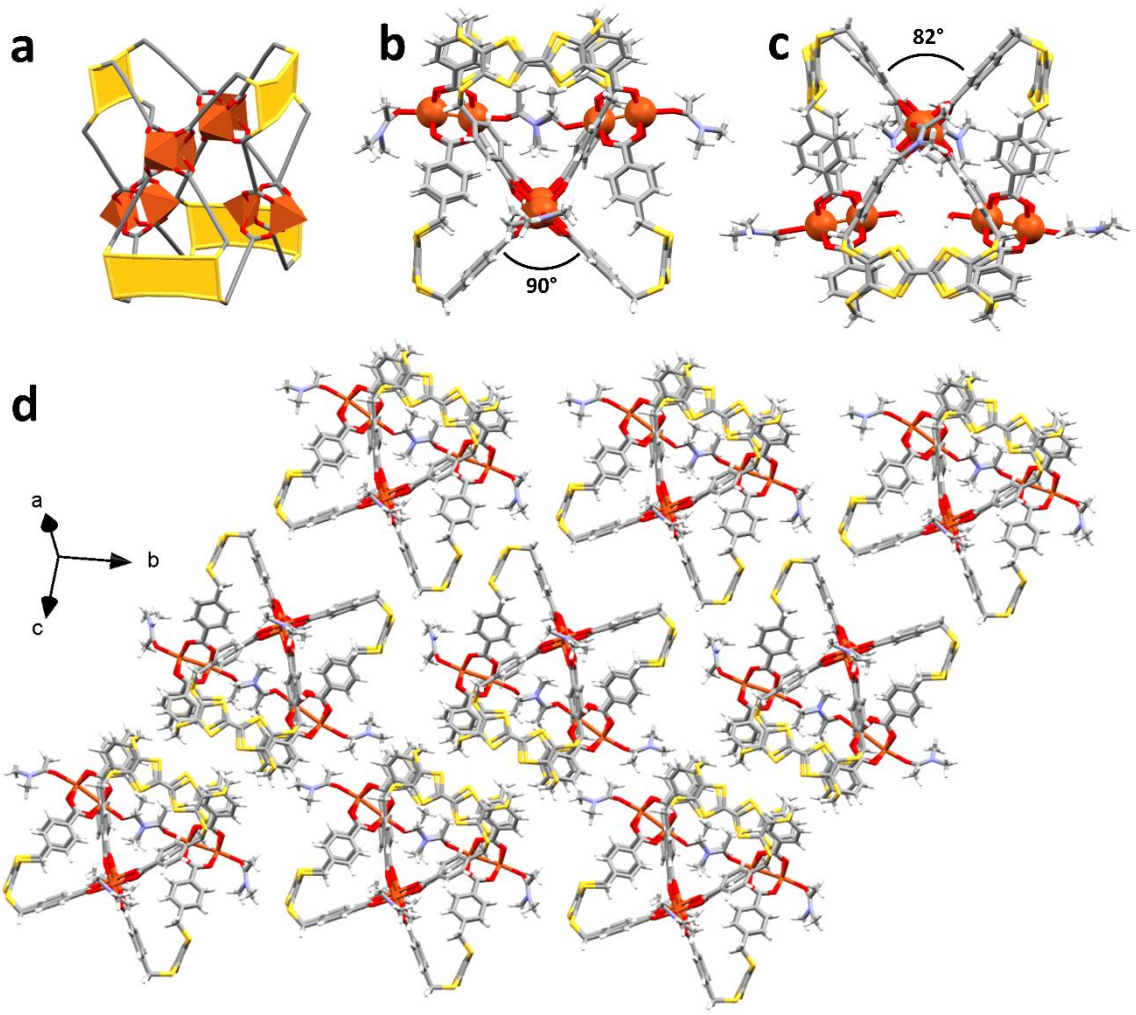

Figure 3. X-ray crystal structure of **Cu_8L_4-(DMAc)** with a) a schematic representation of the cage (yellow = TTF planes and orange = metal paddlewheels), b) and c) two different side views of a cage and d) view of one layer of cages in the packing. Non-coordinated and disordered DMAc molecules were removed for the sake of clarity (Copper: orange ; Carbon: grey ; Oxygen : red ; Sulfur : yellow ; Hydrogen : white).

A similar cage is obtained in DMF. **Cu_8L_4-(DMF)** crystallizes as small green needles in the monoclinic $P2_1/m$ space group. The lesser stability of the crystals upon air exposure prevented the acquisition of a high quality dataset (**see ESI Table 1**). The asymmetric unit contains half of a cage, and the complete formula for one cage is **$Cu_8L_4(H_2O)_8\cdot(DMF)_{1.16}$**. Herein, all of the inner and outer apical positions are occupied by water molecules, and two DMF solvent molecules with partial occupancies of 33% and 25% are crystallographically observed in the structure. The overall cage structure remains the same as for the **Cu_8L_4-(DMAc)** cage, as observed from their superimposition (**Figure 4a**, with **Cu_8L_4-(DMF)** in green and **Cu_8L_4-(DMAc)** in orange). The angles between the planes defined by the aromatic moieties remains in the same range at *ca*. 80-85° (**Figure 4b and c**). H-bonds of the inner H_2O molecules are

observed for two water molecules facing each other, with d_{O-O} in the 3.7 Å range. The central C=C bonds of the TTF moieties stands within the 1.16(3) to 1.29(1) Å range. As this bond length is depending on the TTF redox state, and that no counter-ions are observed in the structure, a neutral form of the TTF moiety is suggested.

The packing differs noticeably from **Cu_8L_4-(DMAc)**, as two adjacent cages interact through H-bonding of H_2O molecules with d_{O-O} = 2.7 Å (**Figure 4d**, blue dashed bonds for H-bonds) and that two TTF moieties from two different cages are p-stacked, with S-S intercage distances down to 3.4 Å (**Figure 4d**, orange dashed bonds for π-π stacking). In the packed structure, 1D channels are defined between the cages with a size of 4 x 9 Å (**Figure 4e**). These are filled with disordered electronic density which was removed using the Solvent Mask function of the Olex2 suite.[33] The weak inter-cage interactions and the 39% solvent occupied volume explain the lack of stability of the cages upon desolvation.

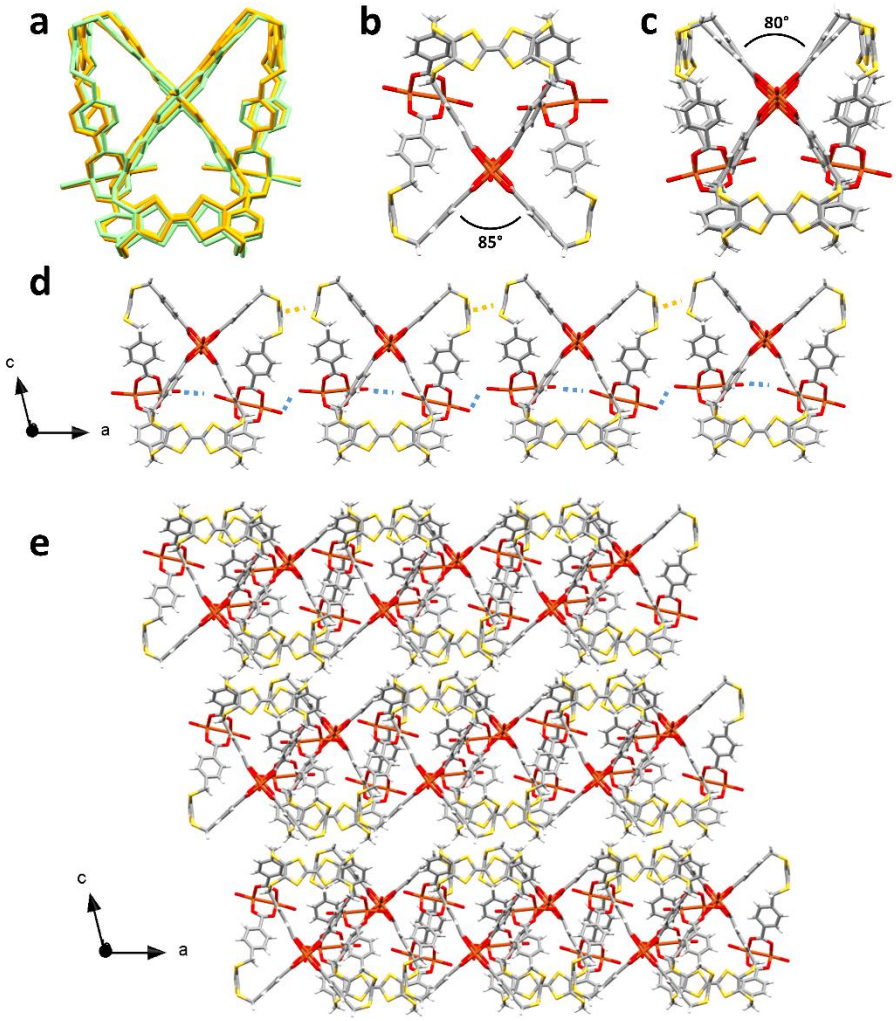

Figure 4. X-ray crystal structure of **Cu_8L_4-(DMF)**. (a) Superimposition of the structures of **Cu_8L_4-(DMAc)** (orange) and **Cu_8L_4-(DMF)** (green). (For (b), (c), (d) and (e) : Copper: orange ; Carbon: grey ; Oxygen : red ; Sulfur : yellow ; Hydrogen : white).

The desolvation and stability of crystals of **Cu_8L_4-(DMAc)** and the **Cu_8L_4-(DMF)** cages were monitored by TGA and PXRD (**see ESI**). They display a rapid loss of solvent below 200 °C that arises from the loss of non-coordinated solvent molecules. The coordinated solvent molecules are lost at higher temperatures and give several weight loss steps until 400 °C. They become amorphous upon desolvation, drying or acetone washing as monitored by PXRD (**see ESI**). The crystals are insoluble in common organic solvents.

Electrochemical properties of **Cu_8L_4-(DMF)** and **Cu_8L_4-(DMAc)** were investigated by solid state cyclic voltammetry. In both cases a quasi-reversible oxidation wave is observed (**Figure 5**, **Cu_8L_4-(DMF)** : $E_1^{1/2}$ = + 0.58 V and **Cu_8L_4-(DMAc)** : $E_1^{1/2}$ = + 0.58 V vs. Ag/AgCl). This wave correspond to the first oxidation

to the radical cation. A second non-reversible oxidation process corresponding to the formation of the dication was observed at higher anodic potentials in both cases (**Cu_8L_4-(DMF)** : E_2^{PA} = + 0.93 V and **Cu_8L_4-(DMAc)** : E_2^{PA} = + 0.98 V vs. Ag/AgCl), resulting in the complete loss of system reversibility (**see SI**).

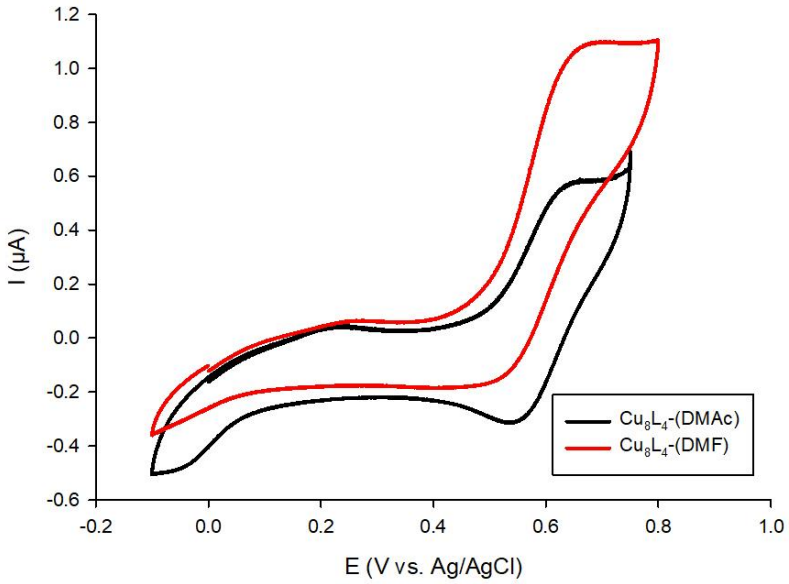

Figure 5. Solid-state cyclic voltammograms for **Cu_8L_4-(DMF)** (red) and **Cu_8L_4-(DMAc)** (black) recorded between -0.1 V and 0.8 V (WE: Pt; CE: Pt wire; RE: Ag/AgCl; electrolyte : 0.1 M $TBAPF_6$ in CH_3CN ; scan rate: 20 $mV.s^{-1}$).

In conclusion, the synthesis and characterization of a new highly flexible ligand bearing an electroactive tetrathioalkyl-TTF core was performed. Its redox activity was assessed by cyclic voltammetry and is similar to the parent molecule TMT-TTF. Despite its high degree of freedom, a cage was self-assembled from **L** with Cu(II) paddlewheel linkers from two different solvent systems. The structures displayed solvent accessible volumes both inside and outside the cages in the solid state. Thanks to the four redox-active moieties per cage, up to 8 e^- per cage could in theory be exchanged, and one can expect large size variations upon expansion of the cage in solution through the breaking of the internal H-bonding system. Solid-state cyclic voltammetry proved that the MOPs retained partially a reversible redox activity in the bulk. Further works are ongoing to solubilize the cages by using other metal centers such as Cr(II), Mn(II) or Rh(II) and using functionalized imidazolates to occupy the external apical paddlewheel positions and increase the cage solubility in common organic solvents.[17,34]

Experimental Part

All reagents and chemicals commercially available were used without further purification. Solvents were dried using standard techniques. NMR spectra were recorded on a Bruker III 300 (^{1}H, 300 MHz ;

^{13}C, 75 MHz). Chemical shifts are given in parts per million (ppm) relative to TMS and coupling J in Hertz (Hz). High resolution mass spectrometry (HRMS) was performed with Jeol JMS-S3000 SpiralTOF. Cyclic voltammetry was performed using a Biologic SP-150 potentiostat with positive feedback compensation. Samples were dissolved in DMF HPLC grade. Tetrabutylammonium hexafluorophosphate (0.1 M as supporting electrolyte) was purchased from Sigma-Aldrich and recrystallized prior to use. Experiments were carried out in a one-compartment cell equipped with platinum working microelectrode (Ø = 2 mm) and a platinum wire counter electrode. A silver wire immersed in 0.01M $AgNO_3$ acetonitrile solution was used as pseudo-reference electrode and checked against ferrocene/ferrocenium couple (Fc/Fc^+) before and after each experiment. Solid state electrochemical behavior of both cages Cu8L4-(DMF) et Cu8L4-(DMAc) were measured with a Biologic SP-150 potentiostat at room temperature using argon bubbled solvent in a three-electrodes set-up. Measurement was carried out using a glass cylinder where a platinum (Pt) electrode (disk diameter = 2mm) used as a working electrode (WE) is placed upside down at the bottom of the glassware. A Pt wire and Ag/AgCl electrodes were used as a counter electrode (CE) and reference electrode (Ref) respectively. The electrolytic solution (TBAPF6 C = 0.1 M, acetonitrile) was placed inside the glass cylinder and the CE and Ref electrodes were immersed into the electrolytic solution. Cages were placed over the WE with a cage-Nafion paste prepared beforehand, Nafion acts as a protective, conductive matrix. All experiments were performed at 20 mV/s (**see SI**). Single crystals of the compounds were mounted on glass fibre loops using a viscous hydrocarbon oil to coat the crystal and then transferred directly to cold nitrogen stream for data collection. Data collection were performed on an Agilent Supernova with CuKα (λ = 1.54184 Å). The structures were solved by intrinsic phasing and refined on F^2 by full matrix least-squares techniques with SHELX programs (SHELXT 2018/2 and SHELXL 2018/3)[35–37] using the ShelXle and the Olex2 graphical user interfaces.[33,38] These data can be obtained free of charge from CCDC, 12 Union road, Cambridge CB2 1EZ, UK with the deposition numbers 2310795-2310797 (e-mail: deposit@ccdc.cam.ac.uk or http://www.ccdc.cam.ac.uk).

Tetramethyl 4,4',4'',4'''-(([2,2'-bi(1,3-dithiolylidene)]-4,4',5,5'-tetrayltetrakis(sulfanediyl))tetrakis(methylene))tetrabenzoate (2)

In a Schlenk tube under an argon atmosphere, **1** (521 mg, 0.95 mmol, 1 equiv.) was suspended in 30 mL EtOH. A freshly prepared sodium ethanolate solution (190 mg Na in 10 mL of EtOH, 8.26 mmol, 8.7 equiv.) was added dropwise into the suspension of **1**. After 3h at RT, methyl 4-(bromomethyl)benzoate (1.09 g, 4.78 mmol, 5.0 equiv.) was added to the dark solution, and an orange precipitate forms readily. After a night at RT, the precipitate was filtrated on a sintered glass funnel and washed by EtOH and Et_2O, yielding the product **2** as an orange powder (0.73 g, 83 %).

^{1}H NMR (300 MHz, Chloroform-*d*) δ 7.98 (d, *J* = 8.2 Hz, 8H), 7.30 (d, *J* = 8.2 Hz, 8H), 3.89 (s, 12H), 3.87 (s, 8H).

^{13}C NMR (75 MHz, Chloroform-*d*) δ 166.86, 141.97, 130.07, 129.58, 129.42, 129.18, 110.61, 77.16, 52.33, 40.45.

MALDI-TOF MS : m/z=924.0 (calcd : 925.25)

HR-MS (M) for $C_{42}H_{36}O_8S_8$: 924.0170 (calcd :924.0176)

4,4',4'',4'''-(([2,2'-bi(1,3-dithiolylidene)]-4,4',5,5'-tetrayltetrakis(sulfanediyl))tetrakis(methylene))tetrabenzoic acid (L)

In a Schlenk tube under an argon atmosphere, the compound **2 (**500 mg, 0.54 mmol, 1 equiv.) was suspended in a THF/MeOH/H_2O mixture (1/1/1 v/v/v, 9 mL). NaOH (216 mg, 5.4 mmol, 10 equiv.) was added and reaction was stirred overnight at 80 °C. Water was added to the reaction until complete dissolution of the media and the resulting solution was heated for a further 30 min at 80 °C. After going back to room temperature, MeOH and THF were removed under reduced pressure. The resulting solution was acidified to pH = 2 using a 10 % HCl solution. The orange precipitate was filtrated on a sintered glass funnel. The obtained solid was washed by H_2O, EtOH and Et_2O. The product **L** was obtained as a dark brown solid (395 mg, 84 %).

^{1}H NMR (300 MHz, DMSO-d_6) δ 12.95 (s, 4H), 7.89 (d, *J* = 8.3 Hz, 8H), 7.34 (d, *J* = 8.3 Hz, 8H), 4.00 (s, 8H).

^{13}C NMR (75 MHz, DMSO-d6) δ 167.01, 142.01, 129.89, 129.53, 129.12, 128.67, 109.57, 39.52, 30.70.

MALDI-TOF MS : m/z= 868.1 (calcd : 869.14)

HR-MS (M) for $C_{38}H_{28}O_8S_8$: 867.9544 (calcd :867.9550)

Synthesis of TTF-CuMOP

L (17 mg, 0.02 mmol) was dissolved in 4 mL of DMF or DMAc. $Cu(AcO)_2$ (3.6 mg, 0.02 mmol) was dissolved in 4 mL of DMF or DMAc. The ligand solution was carefully layered over the metal solution into a solvothermal bomb. After 2 days at 85 °C, the target materials were obtained as thick green needles with 30% and 33% yields respectively.

Elemental analysis Cu_8L_4-(DMAc) $C_{164}H_{133}N_3Cu_8O_{38}S_{32}$,$(H_2O)_{11}$ Theo.: %C, 43.60; %H, 3.46; %N, 0.93; %S, 22.71 / Found: %C, 42.44; %H, 3.28; %N, 1.66; %S, 21.69.

Elemental analysis Cu_8L_4-(DMF) $C_{152}H_{112}Cu_8O_{40}S_{32},(H_2O)_{20}$ Theo.: %C, 40.81; %H, 3.43; %S, 22.94. Found: %C, 39.34; %H, 2.91; %S, 22.32.

Acknowledgements

This work was supported in France by the CNRS and the University of Angers. This work received financial support under the EUR LUMOMAT project and the Investments for the Future program ANR-18-EURE-0012 (support to Y.C. - POEMs project).

References

1 C. J. Pedersen, *Angew. Chem. Int. Ed.*, 1988, **27**, 1021–1027.
2 D. J. Cram, *Angew. Chem. Int. Ed.*, 1988, **27**, 1009–1020.
3 J.-M. Lehn, *Angew. Chem. Int. Ed.*, 1988, **27**, 89–112.
4 S. M. Stagg, C. Gürkan, D. M. Fowler, P. LaPointe, T. R. Foss, C. S. Potter, B. Carragher and W. E. Balch, *Nature*, 2006, **439**, 234–238.
5 G. Vernizzi and M. Olvera de la Cruz, *Proc. Natl. Acad. Sci. USA*, 2007, **104**, 18382–18386.
6 J.-M. Lehn, *Science*, 2002, **295**, 2400–2403.
7 H. Vardhan, M. Yusubov and F. Verpoort, *Coord. Chem. Rev.*, 2016, **306**, 171–194.
8 T. Tateishi, M. Yoshimura, S. Tokuda, F. Matsuda, D. Fujita and S. Furukawa, *Coord. Chem. Rev.*, 2022, **467**, 214612.
9 S. Mollick, S. Mukherjee, D. Kim, Z. Qiao, A. V. Desai, R. Saha, Y. D. More, J. Jiang, M. S. Lah and S. K. Ghosh, *Angew. Chem. Int. Ed.*, 2019, **58**, 1041–1045.
10 S. Furukawa, N. Horike, M. Kondo, Y. Hijikata, A. Carné-Sánchez, P. Larpent, N. Louvain, S. Diring, H. Sato, R. Matsuda, R. Kawano and S. Kitagawa, *Inorg. Chem.*, 2016, **55**, 10843–10846.
11 G. R. Lorzing, B. A. Trump, C. M. Brown and E. D. Bloch, *Chem. Mater.*, 2017, **29**, 8583–8587.
12 Y. Ke, D. J. Collins and H.-C. Zhou, *Inorg. Chem.*, 2005, **44**, 4154–4156.
13 M. Yoshizawa, M. Tamura and M. Fujita, *Science*, 2006, **312**, 251–254.
14 M. Yoshizawa, J. K. Klosterman and M. Fujita, *Angew. Chem. Int. Ed.*, 2009, **48**, 3418–3438.
15 M. Jung, H. Kim, K. Baek and K. Kim, *Angew. Chem. Int. Ed.*, 2008, **47**, 5755–5757.
16 A. Mallick, B. Garai, D. D. Díaz and R. Banerjee, *Angew. Chem. Int. Ed.*, 2013, **52**, 13755–13759.
17 A. Carné-Sánchez, G. A. Craig, P. Larpent, V. Guillerm, K. Urayama, D. Maspoch and S. Furukawa, *Angew. Chem. Int. Ed.*, 2019, **58**, 6347–6350.
18 A. C. Sudik, A. R. Millward, N. W. Ockwig, A. P. Côté, J. Kim and O. M. Yaghi, *J. Am. Chem. Soc.*, 2005, **127**, 7110–7118.
19 D. Lorcy, N. Bellec, M. Fourmigué and N. Avarvari, *Coord. Chem. Rev.*, 2009, **253**, 1398–1438.
20 S. Goeb, S. Bivaud, V. Croué, V. Vajpayee, M. Allain and M. Sallé, *Materials*, 2014, **7**, 611–622.
21 S. Goeb and M. Sallé, *Acc. Chem. Res.*, 2021, **54**, 1043–1055.
22 R. Gasiorowski, T. Jorgensen, J. Møller, T. K. Hansen, M. Pietraszkiewicz and J. Becher, *Adv. Mater.*, 1992, **4**, 568–570.
23 P. Blanchard, N. Svenstrup, J. Rault-Berthelot, A. Riou and J. Becher, *Eur. J. Org. Chem.*, 1998, **1998**, 1743–1757.
24 T. Akutagawa, Y. Abe, Y. Nezu, T. Nakamura, M. Kataoka, A. Yamanaka, K. Inoue, T. Inabe, C. A. Christensen and J. Becher, *Inorg. Chem.*, 1998, **37**, 2330–2331.
25 G. Szalóki, V. Croué, M. Allain, S. Goeb and M. Sallé, *Chem. Commun.*, 2016, **52**, 10012–10015.
26 S. M. Jansze, M. D. Wise, A. V. Vologzhanina, R. Scopelliti and K. Severin, *Chem. Sci.*, 2017, **8**, 1901–1908.
27 J. Olivier, S. Golhen, R. Świetlik, O. Cador, F. Pointillart and L. Ouahab, *Eur. J. Inorg. Chem.*, 2009, **2009**, 3282–3290.
28 D. Bechu, N. Kyritsakas, M. W. Hosseini and S. A. Baudron, *Polyhedron*, 2021, **198**, 115047.
29 H. Nishikawa, Y. Misaki, T. Yamabe and M. Shiro, *Synth. Met.*, 1999, **102**, 1693–1694.
30 P. Guionneau, C. J. Kepert, G. Bravic, D. Chasseau, M. R. Truter, M. Kurmoo and P. Day, *Synth. Met.*, 1997, **86**, 1973–1974.
31 M. Vicent-Morales, M. Esteve-Rochina, J. Calbo, E. Ortí, I. J. Vitórica-Yrezábal and G. Mínguez Espallargas, *J. Am. Chem. Soc.*, 2022, **144**, 9074–9082.
32 K. O. Kirlikovali, S. Goswami, M. R. Mian, M. D. Krzyaniak, M. R. Wasielewski, J. T. Hupp, P. Li and O. K. Farha, *ACS Materials Lett.*, 2022, **4**, 128–135.
33 O. V. Dolomanov, L. J. Bourhis, R. J. Gildea, J. a. K. Howard and H. Puschmann, *J. Appl. Cryst.*, 2009, **42**, 339–341.

34 E. Sánchez-González, M. Y. Tsang, J. Troyano, G. A. Craig and S. Furukawa, *Chem. Soc. Rev.*, 2022, **51**, 4876–4889.
35 G. M. Sheldrick, *Acta Crystallogr. A*, 2008, **64**, 112–122.
36 G. M. Sheldrick, *Acta Crystallogr. A*, 2015, **71**, 3–8.
37 G. M. Sheldrick, *Acta Crystallogr. C*, 2015, **71**, 3–8.
38 C. B. Hübschle, G. M. Sheldrick and B. Dittrich, *J. Appl. Cryst.*, 2011, **44**, 1281–1284.